J. Fluid Mech. (2002), *vol.* 471, *pp.* 159–168.
DOI: 10.1017/S0022112002002161 Printed in the United Kingdom

On the persistence of trailing vortices

By LAURENT JACQUIN AND CARLOS PANTANO†

Department of Fundamental and Experimental Aerodynamics, ONERA
92190 Meudon, France

(Received 15 April 2002 and in revised form 31 July 2002)

The short-wave stability properties of a Batchelor vortex are used to explain the intrinsic resistance of vortices to turbulent diffusion. We show that turbulence produced within the vortex core has to overcome a stabilizing 'dispersion buffer', where energy of the perturbations is dispersed by inertial waves without interfering with the mean flow, before they can reach the periphery of the vortex. While angular momentum is maintained by this mechanism, the difference in energy extraction by turbulence from the axial and tangential velocity fields due to a lack of alignment between the mean and turbulent strain tensors, a typical effect of flow rotation or curvature, leads to stabilization through a progressive damping of the axial shear in the vortex core. We show that the efficiency of these stabilizing mechanisms depends on the swirl number, the ratio between the maximum tangential velocity and the axial velocity difference. If the swirl parameter is low enough, turbulence is able to reach the vortex periphery and a small circulation overshoot develops, leading to weak diffusion of angular momentum outward.

1. Introduction

A large body of experimental evidence shows that the wake vortices generated by a lifting wing are usually very persistent, see e.g. Spalart (1998). They can only be substantially perturbed by cooperative instabilities which result from the interaction with neighbouring vortices. In the case of a single pair of vortices a distance b apart, with equal or opposite circulation Γ and the same characteristic diameter, a, cooperative instabilities are responsible for long- and short-wave instabilities, with wavelengths of order b and a, respectively. The long-wave instability leads to the connection of the vortices and to changes in the flow topology, Crow (1970), whereas the short-wave instability distorts the vortices, Tsai & Widnall (1976). Short waves are also responsible for the merging of co-rotating vortices at high Reynolds number when the aspect ratio a/b is large enough (Le Dizès & Laporte 2002). When there are more than two vortices, cooperative instabilities also develop and may trigger the rapid disorganization of the vortex system, thought to be a possible mechanism for accelerating the decay of aircraft wake vortices (Crouch 1997; Rennich & Lele 1998; Fabre, Jacquin & Loof 2002).

The time required for a cooperative instability to develop is of order $\tau_b = (2\pi b^2)/\Gamma$. When $a \ll b$, that is when the vortices are far from each other, if turbulence is present in the vortex core or at its periphery, significant turbulent diffusion could take place on the time scale $\tau_a = (2\pi a^2)/\Gamma$, which characterizes the convection time in the physical

† Current address: Graduate Aeronautical Laboratories, California Institute of Technology, MC 205-45, Pasadena, CA 91125, USA.

scale of the individual vortex. This may occur before any significant cooperative instability develops. Three sources of turbulence may be considered. The first is the lifting body wake which rolls up into the lift vortices. The propulsive jets may also contribute in the case of an aircraft. These perturbations are somehow ingested by the vortices during the roll-up of the wake. Secondly, turbulence may develop inside the vortices through local instability mechanisms. For instance, a centrifugal instability may develop if vorticity changes sign somewhere, and helical instabilities may appear under the action of a significant axial flow. Lastly, turbulence may be present in the ambient flow. In this case, turbulence macro-scales may contain vorticity of the order of that in the vortices, and the vortices are thus rapidly destroyed. Except in this last case, one must indeed ask why vortices are so resistant to turbulent transport of angular momentum and why the evolution of turbulence does not follow the traditional patterns encountered in free shear flows. There are two possible explanations: either turbulence cannot survive in vortices or alternatively, even if it is present, turbulence cannot transport angular momentum in or out of the vortex. From inspection of the available measurements on lift vortices, one cannot say unambiguously if they are laminar or turbulent because there is considerable uncertainty due to spatial integration problems in the measurements and difficulties in discriminating turbulence from vortex meandering (Devenport *et al.* 1996; Jacquin *et al.* 2001). But we anticipate that the vortex resistance to turbulent spreading is the mark of strong stabilizing effects imposed on turbulence by the flow rotation. Understanding this problem is a key issue for numerical computation and modelling of flows containing lift vortices, Zeman (1995), and for vortex control applications. The basic mechanisms thought to be responsible for the strong stability of vortex flows are explained by considering successively the linear properties of a Batchelor vortex, DNS and experimental results.

2. The stabilizing effect of rotation in a vortex

The main mechanism that must be accounted for to understand turbulence in a vortex is the coupling between rotation and shear. To this end, it may be useful to consider an analogy between a two-dimensional vortex and a shear flow in solid body rotation using a cylindrical coordinate system (r, θ, z) where the velocity components are (U, V, W). In a vortex with no axial velocity, $W = 0$, turbulence is subjected to a shear rate $S = r\mathrm{d}(V/r)/\mathrm{d}r$. This would correspond to the relative vorticity of a rotating shear layer. Superposed on this field is an entrainment vorticity $2V/r$. The sum is the total, or absolute vorticity, $\omega = S + 2V/r = (1/r)\,\mathrm{d}(rV)/\mathrm{d}r$. We know from Lord Rayleigh's work that such a flow becomes locally unstable as soon as the sign of ω changes somewhere in the flow. In this case, a centrifugal instability occurs. From the linearized Euler equations in which perturbations are considered proportional to $\exp(\mathrm{i}kz)\exp(\sigma t)$, it may be shown, see Ash & Khorrami (1995), that in the limit of large k, the square of the temporal amplification rate of these instabilities is

$$\sigma^2(r) = -\frac{2V}{r}\omega = -\frac{1}{r^3}\frac{\mathrm{d}\Gamma^2(r)}{\mathrm{d}r}, \tag{2.1}$$

where k is the streamwise wavenumber. In (2.1), $\Gamma(r) = rV$ is the angular momentum, or circulation (the factor 2π is omitted) of the vortex at radius r. This criterion is a particular case of a more general criterion for centrifugal-type instabilities which holds in incompressible inviscid planar basic flows in a rotating frame and which was established by Sipp & Jacquin (2000). If $\sigma^2 > 0$ the flow is unstable; if $\sigma^2 < 0$

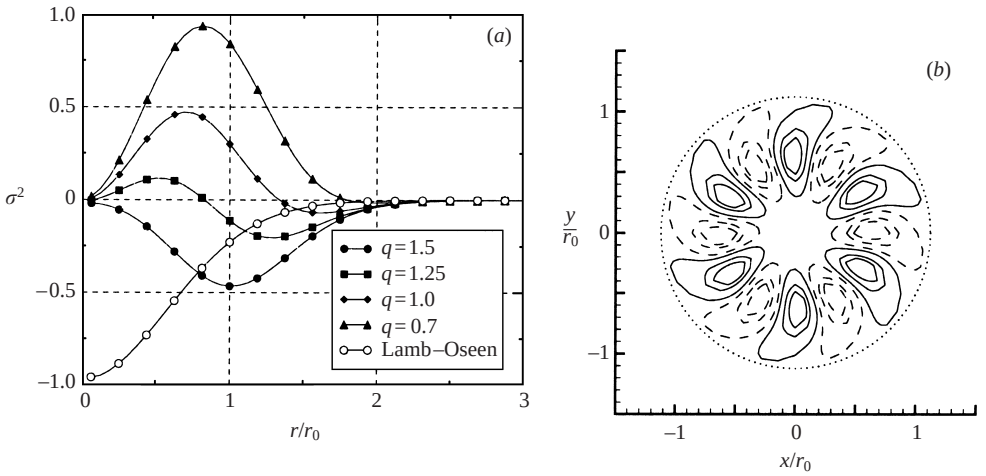

FIGURE 1. (*a*) Amplification rate $\sigma^2(r)$ of short-wave instabilities in a Batchelor vortex for $q = 1.5$, 1.25, 1, 0.7 and in a Lamb–Oseen vortex ($q = \infty$); (*b*) axial (z-component) vorticity fluctuation field of the most amplified ring mode, i.e. $|m| = 6$, for $q = 1$ and $Re = 2000$. In (*a*) $\sigma^2(r)$ is non-dimensionalized with V_0 and r_0 and values are divided by 10 for the Lamb–Oseen case. In (*b*), the dotted and solid lines correspond to vorticity of opposite sign. The dotted circle corresponds to the radius $r = 1.121r_0$ where $V = V_0 = V_{max}$.

the flow is stable. In the latter case, perturbations are transformed into an inertial wave regime which propagates in the vortex axis direction. Here, the expressions for σ corresponding to the two equalities in (2.1) show the similitude between the principle of 'stratification' of a shear flow by streamline curvature or by rotation, as described by Bradshaw (1969), and the classical centrifugal instability. The first leads to the Bradshaw–Richardson criterion (first equality) and the second the Rayleigh criterion (second equality). Both expressions show that a centrifugal instability occurs whenever ω changes sign somewhere. The Rayleigh criterion also shows that this corresponds to an overshoot in the circulation profile ($\Gamma \, \mathrm{d}\Gamma/\mathrm{d}r < 0$). A particle displaced within such a region will be expelled outward or inward due to an excess or a deficit of angular momentum.

We turn our attention to a widely used model for axisymmetric vortices with no axial velocity, the Lamb–Oseen vortex, with tangential velocity given by

$$V = \frac{\Gamma_0}{2\pi r}(1 - \exp(-r^2/r_0^2)), \tag{2.2}$$

where r_0 denotes the initial vortex radius and $\Gamma_0 = \lim_{r\to\infty} 2\pi r V(r)$ is the vortex circulation. The initial peak tangential velocity is denoted by $V_0 = V_{max}$. As shown in figure 1(*a*), in a Lamb–Oseen vortex, the amplification rate σ is everywhere purely imaginary which means that any perturbation will be dispersed into an inertial wave regime with a frequency $|\sigma|$ that increases towards the axis. This property, which is responsible for the dispersion of the perturbations, prevents the vortex from developing turbulence and protects its core from the influence of external perturbations. At the periphery the flow is neutral and becomes a potential flow. Now, if an axial flow is present, for instance a Gaussian jet or wake, with axial velocity respectively given by

$$W = W_0 \pm \Delta W \exp(-r^2/r_0^2), \tag{2.3}$$

the instability properties of the flow change drastically. Equations (2.2) and (2.3) correspond to a Batchelor vortex (Batchelor 1964), an asymptotic solution of a spatially evolving vortex with an axial velocity excess or deficit. This flow is an excellent idealized problem to study vortices with an axial velocity difference in situations where the vortex behaves as a slender cylindrical flow. Here we neglect the mean axial pressure gradient that exists in the spatially evolving vortex, a reasonable hypothesis in several practical cases. The stability properties of the Batchelor vortex are now well-established. At a sufficiently high Reynolds number, the stability is controlled by the value of the swirl parameter, q, defined as

$$q = \frac{\Gamma_0}{2\pi r_0 \Delta W} \approx 1.56 \frac{V_0}{\Delta W}, \tag{2.4}$$

which measures the relative tangential and axial velocity intensity. The inviscid stability theory considers perturbations proportional to $\exp \mathrm{i}(kz + m\theta)\exp(\sigma t)$ with m the azimuthal wavenumber. It shows that the Batchelor vortex is unstable with respect to azimuthal wavenumbers $m < 0$ for small enough swirl, q. The limit value of q, given by Mayer & Powell (1992), Ash & Khorrami (1995) and Fabre & Jacquin (2002), is approximately 1.5. For larger values, rotation stabilizes all perturbations in an inviscid flow. More precisely, the perturbations are transformed into a regime of inertial waves. Among the results of these stability studies, Leibovich & Stewartson (1983) obtained an asymptotic instability criterion expressed as

$$\sigma^2(r) = \frac{2V(r)(r\,\mathrm{d}V/\mathrm{d}r - V)(V^2/r^2 - (\mathrm{d}V/\mathrm{d}r)^2 - (\mathrm{d}W/\mathrm{d}r)^2)}{(r\,\mathrm{d}V/\mathrm{d}r - V)^2 + (r\,\mathrm{d}W/dr)^2}. \tag{2.5}$$

A necessary condition for local instability is $\sigma^2(r) > 0$. Leibovich & Stewartson's (1983) analysis shows that, in the limit $k \to \infty$, if there is a radius r where $\sigma^2 > 0$, one can construct modes which are localized in the vicinity of r and whose amplification rate is equal to σ (ring modes). As a result, if $\sigma^2 > 0$, a short-wave perturbation initially located at radius r is expected to grow and eventually participate in a turbulent regime. On the other hand, if $\sigma^2 < 0$, a perturbation at radius r will not be amplified and will be dispersed. Setting $\mathrm{d}W/\mathrm{d}r = 0$ (for all r) in (2.5) recovers (2.1) so that it becomes appropriate then to view (2.5) as a sort of generalization of the Rayleigh criterion of stability in which the effects of the axial flow are taken into account. Figure 1(a) shows σ^2 versus r for the Batchelor vortex and four different values of the swirl q. For $q = 1.5$, σ^2 is everywhere negative or null and the flow is entirely stable. More precisely, the criterion predicts stability for $q \geqslant \sqrt{2}$ which is close to 1.5. For $q = 1.25$, there is a small region within the core where the flow is unstable with respect to helical modes ($\sigma^2 > 0$). This region extends further for $q = 1$ and it occupies almost the whole flow for $q = 0.7$. A 'ring mode' is shown in figure 1(b) where we have plotted the axial (z-component) vorticity fluctuation field corresponding to the most amplified helical mode, here $|m| = 6$, obtained for $q = 1$ and $Re = 2000$, see Fabre & Jacquin (2002). Figure 1(a) highlights the stabilizing effect of rotation where it is seen that for $0.7 \leqslant q \leqslant 1.5$, the external part of the vortex is surrounded by a 'dispersion buffer', where $\sigma^2(r) < 0$, that is where perturbations are transformed into non-amplified propagating waves. The width of this region decreases with decreasing q, i.e. as the jet or wake becomes stronger. For $q = 0.7$, the 'dispersion buffer' almost vanishes. *We think that the presence of this 'dispersion buffer' is fundamental in explaining why a vortex is inefficient in transporting angular momentum even though its core may contain perturbations.* For $q = 1$, for instance, the perturbations that are produced inside the core around $r/r_0 \approx 0.75$ must cross this stability region before they are able to diffuse

further away. The perturbations are then transformed into neutral waves with a speed that is proportional to $|\sigma|$ with no energy exchange with the basic flow. This zone is responsible for the confinement of turbulence within the core. In the core, the energy of the axial flow is extracted preferentially by the instability and by turbulence (see § 3) whereas in the 'dispersion buffer', where the velocity is mainly tangential, the perturbations transported there propagate without modification of the mean tangential flow. As a result, the axial velocity deficit (wake) or excess (jet) weakens while the angular momentum is maintained; this results in an increase of the swirl $q(t) = \Gamma(t)/(2\pi r_0(t)\Delta W(t))$ which leads to elimination of turbulence production due to increased stability. The LES and DNS calculations of Ragab & Sreedhar (1995), Qin (1998), Sipp, Coppens & Jacquin (1999) and Pantano & Jacquin (2001) confirm this scenario. They show a differential decay of the velocity components, an increase of q and a progressive restabilization of the flow. This scenario is also suggested by few experiments, such as the one that will be revisited in § 3. In the above discussion it was assumed that asymptotic linear stability indicates how turbulence behaves within the flow. An asymptotic short-wave analysis, such as that leading to (2.5), amounts to considering perturbations whose scales are smaller than those of the variation of the mean flow and it describes growing perturbations of infinitesimal initial strength. But this also describes a mechanism which may entertain finite-amplitude perturbations such as those of a fully developed turbulent field superposed on a basic, or Reynolds-averaged, flow. It indicates where turbulent perturbations will be produced when the mean flow remains unstable after saturation of the linear transient.

3. Numerical and experimental evidence

Let us consider the DNS results of Pantano & Jacquin (2001). This simulation corresponds to a DNS of a Batchelor vortex with $q = 1$, starting from quasi-random turbulent fluctuations of small intensity (2% of V_0) using high-order of accuracy finite differences. The resolution is $248 \times 248 \times 284$ grid points with a domain of size $L_1 = L_2 = 64r_0$ and $L_3 = 12.36r_0$ in the axial direction. The Reynolds number based on peak tangential velocity is $Re = V_0 r_0/\nu = 2000$. Further details can be found in Pantano & Jacquin (2001). Figure 2 shows several quantities extracted from this DNS. Figure 2(a) shows the evolution of the volume-integrated turbulent kinetic energy, $\langle k \rangle$, where $\langle k \rangle = \int_0^\infty 2\pi r k(r,t)\,\mathrm{d}r$ is the volume integral of the turbulent kinetic energy, $k(r,t)$. The non-dimensional time is defined as $\tau = tV_0/2\pi r_0$. The same figure shows the evolution of the swirl number, equation (2.4), with time. The level of turbulence fluctuations increases from its initial low level, reaches a maximum at $\tau \approx 4$ and decay gradually thereafter. In accordance with stability analysis the turbulent kinetic energy starts to decrease approximately when the parameter $q(\tau)$ reaches a value of 1.5. This confirms the restabilization of the flow due to the differential decay of the velocity components. As far as turbulence correlations are concerned, this restabilization mechanism may be understood as the result of a lack of alignment between the mean and turbulent strain tensors due to the flow rotation or curvature. Figure 2(b) shows the evolution with time of the integrated correlation between the rate of strain, S_{ij}, and the Reynolds shear stress from the DNS for the angular, $R_{r\theta}$, and axial, R_{rz}, turbulent stresses ($R_{r\theta} = \overline{u_r u_\theta}$ and $R_{rz} = \overline{u_r u_z}$ are the Reynolds stresses, u_r, u_θ and u_z being the velocity fluctuations in the radial, tangential and axial directions). The correlation is defined as $C_{ij} = -\langle R_{ij} S_{ij} \rangle / \sqrt{\langle R_{ij}^2 \rangle \langle S_{ij}^2 \rangle}$ (repeated indexes do not imply summation here). It can be observed that $C_{r\theta}$ is low up to $\tau \simeq 3$ while C_{rz} is always

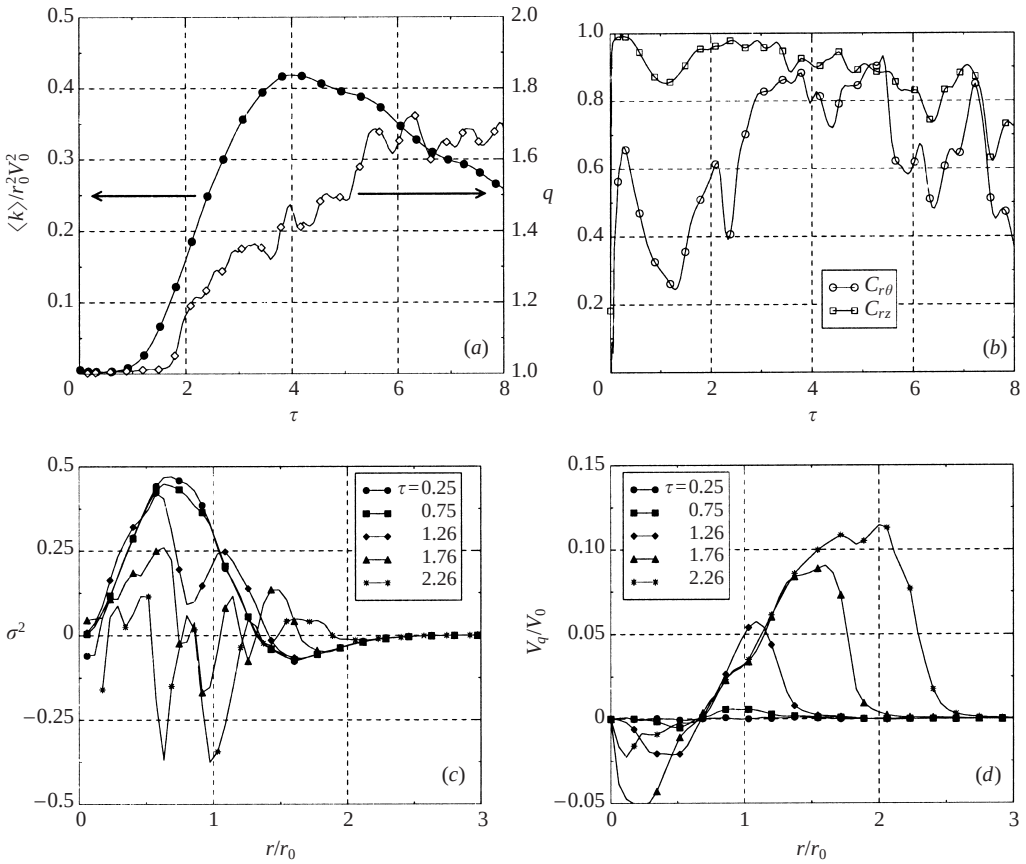

FIGURE 2. (*a*) Volume-integrated turbulent kinetic energy $\langle k\rangle$ and swirl number q; (*b*) Reynolds stress and rate of strain correlation coefficient as a function of time; (*c*) radial distribution of the amplification rate σ^2 of the short-wave instabilities at different times, (*d*) velocity of turbulent transport, V_q, from Pantano & Jacquin (2001).

high, indicating how inefficient angular is with respect to axial turbulent production. This holds during both the linear and the nonlinear regimes. This difference then also holds for dissipation and diffusion which explains why q increases. After $\tau \simeq 3$, the correlation increases but soon thereafter the Reynolds stresses (and turbulence) start to decrease due to the restabilization of the flow.

Figure 2(*c*) shows the temporal evolution of $\sigma^2(r,t)$ calculated from (2.5) by using the averaged velocity profiles extracted from the DNS database. The initial distribution of $\sigma^2(r)$ is close to that shown in figure 1(*a*) where the unstable helical perturbations $m<0$ give rise to a collection of 'ring modes' located around $r/r_0 \approx 0.75$. Then the unstable region breaks in two parts, as a result of a preferential extraction of energy from the axial flow compared to the tangential flow, as discussed above. This holds both in the linear and nonlinear (turbulent) regimes. For the linear regime, this was clearly confirmed by inspection of the Reynolds stresses obtained from a computation of the normal modes extracted from a stability analysis of this flow. It is observed that an unstable region propagates towards the 'dispersion buffer' while the associated amplification rate decays due to stabilizing effects in the 'dispersion buffer' as advocated in the preceding section. But, as shown in figure 2(*c*),

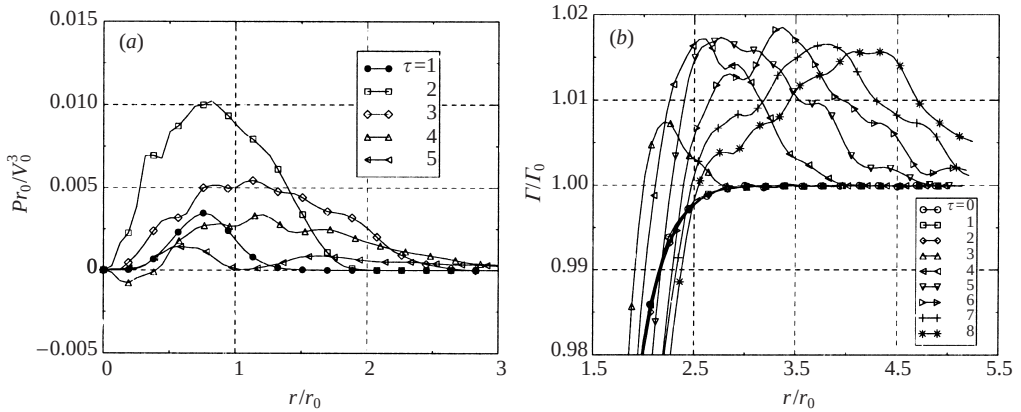

FIGURE 3. (*a*) Radial distribution of the turbulent production, P, and (*b*) circulation showing a 2% overshoot propagating outward, from Pantano & Jacquin (2001).

a small instability region succeeds, beyond $\tau = 2.26$, in reaching the vortex periphery, around $r/r_0 = 2$. This is the result of the accumulation of angular momentum transported by turbulence. Figure 2(*d*) shows the velocity of transport of turbulent kinetic energy $V_q = \overline{u_r u_i u_i}/\overline{u_i u_i}$, see Andreopoulos & Bradshaw (1980), at the same times as figure 2(*c*). It is observed that V_q 'radiates from the instability source' and is well-correlated with the stability prediction of σ^2 in the flow periphery: V_q reaches a maximum value at the location where $\sigma^2 = 0$ and then abruptly vanishes within the 'dispersion buffer', supporting the ideas described in § 2. Figure 3(*a*) shows the turbulent production profiles. At $\tau = 1$, the perturbations grow around $r \approx 0.75 r_0$ in accordance with figure 1(*a*) for $q = 1$. This local energy production, constrained within the core by the 'dispersion buffer' is maintained up to about $\tau \simeq 2$. At $\tau \simeq 3$, production of turbulence has already reached the vortex periphery beyond $r/r_0 = 2$. But this production is smaller than that prevailing during the initial surge ($\tau < 2$). In this region, the axial-flow gradient is small and the instability mechanism that results is a centrifugal instability, see (2.1). The LES and DNS calculations of Ragab & Sreedhar (1995) showed the emergence of a circulation overshoot of small magnitude (2% of Γ_0). This was also observed in the DNS by Qin (1998) and is also clear in figure 3(*b*) obtained from the DNS of Pantano & Jacquin (2001). The propagation of the circulation overshoot illustrated in figure 3(*b*) is the diffusion process by which angular momentum may be finally transported outward, albeit at a very small rate. The peak circulation is subjected to statistical variability due to the nature of turbulence, but the value of 2% is typical and has already be found by Qin (1998). Let us consider this diffusion mechanism. Within the temporal approximation of the Batchelor vortex, the turbulent torque, $r^2 R_{r\theta}$, is the only term that appears in the mean conservation equation of V. One may easily transform this equation into one for the deficit of angular momentum from 0 to r, $J(r,t) = \int_0^r (1 - \Gamma(r,t)/\Gamma_0) r \, \mathrm{d}r$ which is also the second moment of vorticity $J(r,t) = (2\pi/r_0^2\Gamma_0)\int_0^r r^2 \omega r \, \mathrm{d}r$. This equation reads

$$\frac{\partial J(r,t)}{\partial t} = \frac{2\pi}{\Gamma_0} r^2 R_{r\theta}(r,t) + \nu r^3 \frac{\partial}{\partial r}\left(\frac{1}{r^3}\frac{\partial J}{\partial r} - \frac{1}{r^2}\right). \tag{3.1}$$

The $\lim_{r\to\infty} J(r,t) = \bar{r}^2(t)$ represents the (squared) vorticity dispersion radius. From (3.1), it can be verified that $\bar{r}^2(t)$ obeys $\partial \bar{r}^2/\partial t = (2\pi/\Gamma_0) r^2 R_{r\theta}(\infty, t) + 4\nu$, which can be integrated to give $\bar{r}^2(t) = \bar{r}^2(0) + 4\nu t$, if the turbulent torque vanishes at infinity. This

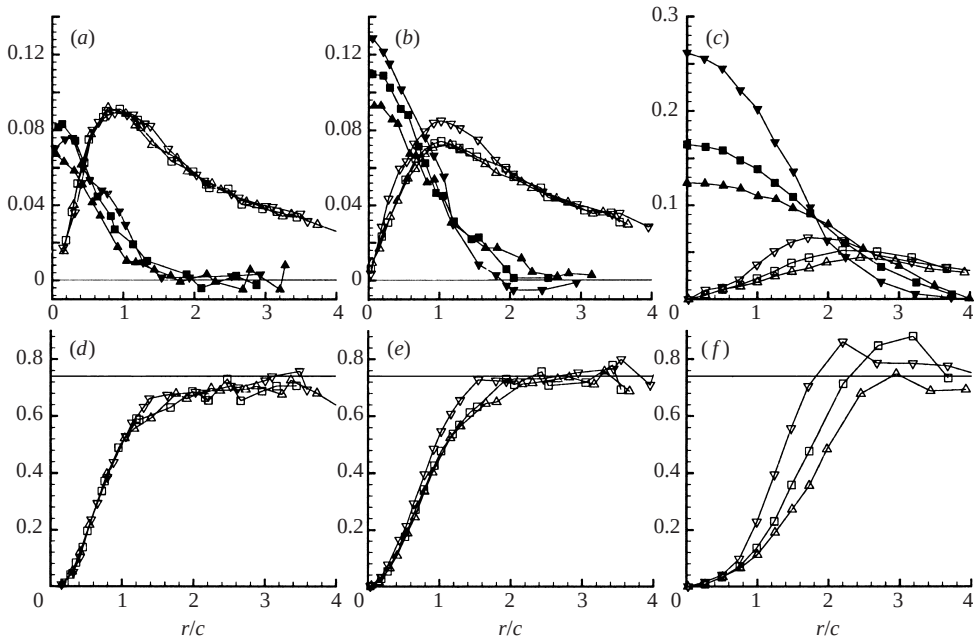

FIGURE 4. Mean flow profiles (top) and circulation (bottom) in three downstream sections behind a split wing: (*a*, *d*) weak jet case B, (*b*, *e*) strong wake case E, (*c*, *f*) strong jet case A; symbols: ∇, $z/c = 45$; $\square$, $z/c = 78$; $\triangle$, $z/c = 109$; open symbols V/W_0 and $\Gamma = 2\pi r V/W_0 c$, solid symbols $\Delta W/W_0$, the total circulation is $\Gamma_0/(W_0 c) \approx 0.74$, from Phillips & Graham (1984).

result implies that the time evolution of the vorticity dispersion radius cannot exceed that of a laminar vortex, which is a well-known and important result, see Saffman (1992). Moreover, (3.1) shows that the first term on the right can lead to the development of a transitory circulation overshoot if turbulence is able to reach the periphery. In this context, Uberoi (1979) points out that even if the flow is initially unstable, there is no reason to believe that it will remain unstable or generate a circulation overshoot. We show here that this depends on the initial value of q: if q is small enough, an overshoot may appear. For $q = 1$, it turns out that the circulation overshoot is very small.

We consider now an experiment carried out by Phillips & Graham (1984) which is one of the rare experiments containing comprehensive data on mean and turbulent quantities in a trailing vortex. It is based on the use of a split wing with a narrow central cylindrical body. This produces a single vortex whose core may be manipulated by introducing a jet or producing a wake (with an obstacle) in the central body region. This experiment was designed to produce a thick vortex core and, in contrast to wing vortices, the vortex so obtained seems to be weakly affected by meandering effects. Three cases among the five considered in this reference are analysed here: a weak jet, a strong wake and a strong jet. They correspond respectively to cases B, E and A in Phillips & Graham (1984). The profiles of the axial velocity difference, ΔW, and of the tangential velocity, V, normalized by the free-stream velocity W_0 are shown for three sections in figure 4(*a–c*). The vortex core in the first measuring section is $r_0 \approx c$ (where c indicates the chord of the vortex-generator wings) for cases B and E, and $r_0 \approx 2c$ for case A. Calculation of the swirl q in the first measurement section using (2.4) gives $q \approx 1.8$ for case B, $q \approx 1.0$ for case E and $q \approx 0.4$ for case A. Case A departs from the others by a very rapid evolution and is discussed later. The

convection length scale for the development of the stability/turbulence mechanisms described in § 2 is $\Delta z/c = (2\pi W_0 r_0)/(V_0 c)$. For cases B and E one obtains $\Delta z(\tau = 1)/c$ close to 70 which means that only one convective time scale τ is separating the first and last measurement sections. Figure 4(*d–f*) shows the circulation deduced from these experimental data. In the first case, the angular momentum remains frozen, see figure 4(*a*, *d*). This is in accordance with the fact that for $q \geqslant 1.5$ the flow is stable and free from any production of turbulence. The measurements indeed show that turbulence is weak. When the flow is forced to smaller q, both the axial and tangential velocity components are changing downstream. In case E, see figure 4(*b*, *e*), the changes are moderate. Angular momentum diffuses a little and the emergence of a small overshoot can be guessed in figure 4(*e*) when compared to figure 4(*d*). The swirl number increases from $q \approx 1$ at $z/c = 45$ to nearly $q = 1.3$ in the last section $z/c = 109$. This agrees with figure 2(*a*) where an increase of the swirl number from $q = 1$, and to 1.3 also occurs within nearly one convective time scale τ. Further evolution towards full stability may be anticipated. For case A, which is characterized by a very low value of q, the flow undergoes a much more dramatic change, see figure 4(*c*,*f*). In particular, a large overshoot is observed and could have travelled away from the measurement region in the last section. Starting from $q \approx 0.4$, a very low value, one finds $q \approx 0.6$ in the last measurement section so that the flow should keep on evolving significantly further downstream. For such low swirl values, one may have to consider other mechanisms than those described above. In particular, due to the rapid axial variation of the flow, the axial and tangential velocity components are in significant interaction through an axial pressure gradient, which puts this case beyond the limit of applicability of a temporal approach such as that considered in this paper. Also, a convective/absolute transition characterizes a Batchelor vortex for such low values of q, see Olendraru & Sellier (2002). However, it may be noted that the evolution of this flow amounts to an amplification of the mechanisms that prevail for mild values of q, i.e. increase of short-wave stability (increase of q) and transport of angular momentum by a circulation overshoot. To sum-up, this experiment shows that a vortex evolves towards an equilibrium state corresponding to $q \geqslant 1.5$ and it then becomes persistent; starting from a low enough value of the swirl parameter q (typically smaller than 1), turbulence may lead to diffusion of angular momentum ensured by a propagating circulation overshoot.

4. Conclusions

Considering a Batchelor vortex, a model for trailing vortices, it is shown that the resistance of vortices to turbulent transport is associated with their short-wave stability properties. Depending on the magnitude of the swirl parameter, q, the turbulence generated at the core has to overcome a 'dispersion buffer' that lies adjacent to the vortex core before turbulent perturbations can reach the periphery of the vortex. When they reach this region, the perturbations are transformed into propagating waves which almost do not interact with the basic tangential field. This, together with the rotation-induced difference in energy extraction by turbulence from axial and tangential velocity fields, result in a progressive damping of the axial shear in the vortex core while angular momentum is maintained; the stability of the flow increases and turbulence is progressively eliminated from the vortex by dissipation. DNS and experimental results are analysed and shown to agree with this conclusion. In the case where the vortex is far from equilibrium, that is when q is small enough, turbulence may succeed in breaking stability and diffusing angular momentum. This

diffusion is only significant for vortices with q smaller than unity. Further investigation of the effects of turbulence in vortices within this regime is needed.

This work was supported by ONERA Federated Research Project on 'Wake Vortex Dynamics'. We are grateful to David Fabre for fruitful comments. A preliminary version was presented in the EUROMECH Colloquium No 433 on 'Dynamics of Trailing Vortices', RWTH Aachen, March 21–22, 2002.

REFERENCES

Andreopoulos, J. & Bradshaw, P. 1980 Measurements of interacting turbulent shear layers in the near wake of a flat plate. *J. Fluid Mech.* **100**, 639–668.

Ash, R. L. & Khorrami, M. R. 1995 Vortex stability. In *Fluid Vortices* (ed. S. I. Green), chap. 8, pp. 317–372. Kluwer.

Batchelor, G. 1964 Axial flow in trailing line vortices. *J. Fluid Mech.* **20**, 645–658.

Bradshaw, P. 1969 *Effects of Streamline Curvature on Turbulent Flow*. AGARD AG-169.

Crouch, J. D. 1997 Instability and transient growth for two trailing-vortex pairs. *J. Fluid Mech.* **350**, 311–330.

Crow, S. 1970 Stability theory for a pair of trailing vortices. *AIAA J.* **8**, 2172–2179.

Devenport, W. J., Rife, M. C., Liaps, S. & Follin, G. J. 1996 The structure and development of a wing tip vortex. *J. Fluid Mech.* **312**, 67–106.

Fabre, D. & Jacquin, L. 2002 Viscous instabilities in trailing vortices at large swirl numbers. Submitted to *J. Fluid Mech.*

Fabre, D., Jacquin, L. & Loof, A. 2002 Optimal perturbations in a four-vortex aircraft wake in counter-rotating configuration. *J. Fluid Mech.* **451**, 319–328.

Jacquin, L., Fabre, D., Geffroy, P. & Coustols, E. 2001 The properties of a transport aircraft wake in the extended nearfield: an experimental study. *AIAA Paper* 2002-1038.

Le Dizès, S. & Laporte, F. 2002 Theoretical predictions for the elliptical instability in a two-vortex flow. *J. Fluid Mech.* **471**, 169–201.

Leibovich, S. & Stewartson, K. 1983 A sufficient condition for the instability of columnar vortices. *J. Fluid Mech.* **126**, 335–356.

Mayer, E. W. & Powell, K. G. 1992 Viscous and inviscid instabilities of a trailing vortex. *J. Fluid Mech.* **245**, 91–114.

Olendraru, C. & Sellier, A. 2002 Viscous effects in the convective/absolute instability of the batchelor vortex. *J. Fluid Mech.* **459**, 371–396.

Pantano, C. & Jacquin, L. 2001 Differential rotation effects on a turbulent batchelor vortex. In *DLES-IV Workshop, Enschede, The Netherlands, July 18–20, 2001*. Kluwer.

Phillips, W. R. C. & Graham, J. A. H. 1984 Reynolds stress measurements in a turbulent trailing vortex. *J. Fluid Mech.* **147**, 353–371.

Qin, J. 1998 Numerical simulations of a turbulent axial vortex. PhD thesis, Purdue University.

Ragab, S. & Sreedhar, M. 1995 Numerical simulations of vortices with axial velocity deficits. *Phys. Fluids* **7**, 549–558.

Rennich, S. C. & Lele, S. K. 1998 A method for accelerating the destruction of aircraft wake vortices. *AIAA Paper* 98-0667.

Saffman, P. 1992 *Vortex Dynamics*. Cambridge University Press.

Sipp, D., Coppens, F. & Jacquin, L. 1999 Theoretical and numerical analysis of wake vortices. *ESSAIM Proc.* **7**, 397–407.

Sipp, D. & Jacquin, L. 2000 Three-dimensional centrifugal-type instabilities of two-dimensional flows in rotating systems. *Phys. Fluids* **12**, 1740–1748.

Spalart, P. 1998 Airplane trailing vortices. *Annu. Rev. Fluid Mech.* **30**, 107–138.

Tsai, C.-Y. & Widnall, S. 1976 The stability of short waves on a straight vortex filament in a weak externally imposed strain field. *J. Fluid Mech.* **73**, 721–733.

Uberoi, M. 1979 Mechanisms of decay of laminar and turbulent vortices. *J. Fluid Mech.* **90**, 241–255.

Zeman, O. 1995 The persistence of trailing vortices: A modeling study. *Phys. Fluids* **7**, 135–143.